

AN ABSTRACT OF THE THESIS OF

Joshua M. Owens for the degree of Bachelor of Science in Bioresource Research presented on December 11, 2002. Title: Comparison of Small-Scale and Field-Scale Saturated Hydraulic Conductivity: A Tale of Cores and Drains.

Abstract approved: \_\_\_\_\_



John S. Selker

Saturated hydraulic conductivity ( $K_s$ ) is a central soil physical property in determining water movement and contaminant transport through soils; hence modeling this system requires an accurate determination of  $K_s$ . Decimeter-scale  $K_s$  measurements employing cores or infiltrometers are used frequently, but field-scale  $K_s$  values are required to encompass the full range of operational flow processes. The objective of this study was to determine the utility of small-scale measurements in describing field-scale permeability.

Four tile-drained fields in the Willamette Valley, Oregon; were studied for drainage rate and contaminant transport from field-applied chemicals to ground water and surface water. Decimeter-scale  $K_s$  was measured using 137  $\text{cm}^3$  undisturbed soil cores collected at depths of 30, 60, 90 and 120 cm. Field-scale  $K_s$  is estimated using a classic solution to the time-dependent non-linear Boussinesq equation developed by Polubarinova-Kochina (P-K) for the shape and evolution of a water table draw down in response to parallel horizontal drains overlaying an impermeable layer. Piezometers were installed along a perpendicular transect crossing two drains to observe water table fluctuations. These data were fitted to the P-K model to determine  $K_s$ . Key observations included a good fit of the observations to the model, and a dramatic permeability

increase, exceeding 10 fold, seen at the field-scale compared to the decimeter-scale. This indicates that transport through soils will occur much faster than estimated using decimeter-scale measurements of  $K_s$ . The P-K approach is a practical, low cost method to obtain field-scale permeability.

Comparison of Small-Scale and Field-Scale Saturated Hydraulic Conductivity: A Tale of  
Cores and Drains

by  
Joshua M. Owens

A THESIS

submitted to

Oregon State University

in partial fulfillment of  
the requirements for the  
degree of

Bachelor of Science

Presented December 11, 2002

Copyright by Joshua Owens December 11, 2002 All rights reserved

Bachelor of Science thesis of Joshua M. Owens presented on December 11, 2002

APPROVED:



---

Faculty Mentor



---

Secondary Faculty Mentor

Oregon State University  
Bioresource Research  
4017 Ag & Life Science  
Corvallis, OR 97331-7304

---

Director of Bioresource Research

I understand that my thesis will become part of the permanent collection of the Bioresource Research program. My signature below authorizes release of my thesis to any reader upon request.



---

Joshua M. Owens, Author

## ACKNOWLEDGEMENTS

I would like to thank:

The Oregon Department of Agriculture for funding.

Kristy Warren for her dedication to the project and all the hard work that she put into it

John Selker and Marshall English for their mentorship

Anita Azarenko, Kate Field and Wanda Crannell for their dedication to the Bioresource Research program and its students

Mike Gangwer for his help with the soil-moisture retention analysis

My fiancée, Cory Ducey, for all of her love and support

My parents, Vyrle and Dolly Owens, for all of their love and support

## TABLE OF CONTENTS

	<u>Page</u>
Introduction.....	1
Literature Review.....	4
Hydraulic Conductivity.....	4
Contaminants in Tile Drains.....	5
Materials and Methods.....	7
Site Descriptions.....	7
Field Instrumentation.....	8
Field-Scale $K_s$ Estimation.....	9
Undisturbed Soil Core Sampling.....	11
Small-Scale $K_s$ Estimation.....	11
Soil-Moisture Retention Curves and Voidable Porosity.....	12
Results and Discussion.....	14
Saturated Hydraulic Conductivity.....	14
Field 1.....	15
Field 2.....	17
Field 3.....	19
Field 4.....	20
Matric Potential and Voidable Porosity.....	29
Bulk Density.....	32
Conclusions.....	34
References.....	36
Appendix A: Soil-moisture Retention Data.....	39

## LIST OF FIGURES

<u>Figure</u>		<u>Page</u>
1.	Correlation for field 1 in the 3 events analyzed	16
2.	Field 1 comparison of field-scale $K_s$ with small-scale $K_s$	16
3.	Correlation for field 2 event 1: method 1	18
4.	Correlation for field 2 event 1: method 2	18
5.	Field 2 comparison of field-scale $K_s$ with small-scale $K_s$	19
6.	Field 3 small-scale $K_s$	20
7.	Correlation for field 4 event 1: method 1	21
8.	Correlation for field 4 event 1: method 2	21
9.	Correlation for field 4 event 2: method 1	22
10.	Correlation for field 4 event 2: method 2	23
11.	Correlation for field 4 event 3: method 1	24
12.	Correlation for field 4 event 3: method 2	24
13.	Field 4 comparison of field-scale $K_s$ with small-scale $K_s$	25
14.	Spring water table draw down in field 2	28
15.	Water table draw down in field 4	29
16.	Field 1 soil-moisture retention from $-3$ kPa to $-300$ kPa	30
17.	Field 2 soil-moisture retention $-3$ kPa to $-300$ kPa	30
18.	Field 3 soil-moisture retention from $-3$ kPa to $-300$ kPa	31
19.	Field 4 soil-moisture retention from $-3$ kPa to $-30$ kPa	31
20.	Soil bulk density for all fields based on depth	33

## LIST OF TABLES

<u>Table</u>		<u>Page</u>
1.	Effect of Drainage on Barley Yield	2
2.	Pressures used for soil-moisture retention curve	13
3.	Ratio of arithmetic mean small- and field-scale $K_s$ (cm/s)	14
4.	Coefficient of Variance (COV) for small- and field-scale $K_s$	14
5.	Comparison of $K_s$ between fields	26
6.	Field 1 desorption soil-moisture retention data	39
7.	Field 2 desorption soil-moisture retention data	39
8.	Field 3 desorption soil-moisture retention data	40
9.	Field 4 desorption soil-moisture retention data	41

# Comparison of Small-Scale and Field-Scale Saturated Hydraulic Conductivity: A Tale of Cores and Drains

## **Introduction**

Saturated hydraulic conductivity ( $K_s$ ) is a central soil physical property in determining water and contaminant transport through soils.  $K_s$  is a key parameter for determining drainage requirements in agricultural soil systems to improve crop yield, as well as to estimate the transport rate of contaminants from the soil surface to the tile drain. Decimeter-scale  $K_s$  measurements employing cores or infiltrometers are used frequently, but field-scale  $K_s$  values are required to encompass the full range of operational flow processes. Tile drains are favorable for hydrologic investigations because they integrate the flow processes that influence transport at a field scale. Estimating  $K_s$  using tile drains is representative of the true hydraulic properties present in fields.

When water lands on a field, by precipitation or irrigation, it is partitioned between infiltration and runoff. Infiltrated water can then leave the soil by evapotranspiration or internal drainage. Evapotranspiration is not significant in the Willamette Valley during winter months due to low incident radiation and high relative humidity; internal drainage is the key mechanism for removing water from these soil profiles in winter. Many of the poorly drained Willamette Valley soils preclude effective internal drainage, potentially remedied by the installation of tile drains.

Tile drains allow water to move through the soil, reducing surface runoff, erosion, and sediment and chemical delivery to surface water. Because water is transported

through the soil column, contaminants are largely removed. Therefore tile drains eliminate water which is visually and chemically much cleaner than surface runoff. (Warren, et al. 2002). However, tile drains have come under increased scrutiny as pathways for surface water contamination. This may be desirable in the Willamette Valley, where tile drains can intercept and export contaminants to surface water that may otherwise pollute ground water. This occurs during high flow periods when surface water contamination is rapidly diluted and removed.

The use of agricultural drain tiles in the Willamette Valley, Oregon is extensive. Many Willamette Valley soils are classified as poorly drained, somewhat poorly drained or moderately well drained. Combined with level topography and wet winter months, this causes standing water and saturated soil profiles extending into the spring in many undrained lands. Saturated conditions stunt growth and reduce yield when growing perennial crops, such as alfalfa. Drained land is available for working earlier in the year, lengthening the growing season for annual crops, warming the soil earlier in spring, and increasing yield. The effect of drainage on barley yield is shown on table 1.

Table 1 Effect of Drainage on Barley Yield, from Powers and King (1950) pg 17

Distance Between Laterals	Bushels yield per acre
25 feet	33.73
50 feet	29.9
75 feet	27.9
100 feet	20.35
Undrained	15

Drainage also facilitates the use of winter cover crops that have recently been used in the Willamette Valley; which in turn protects against erosion, retains nitrogen in the soil, can be used as green manure, and can increase the frequency that high value

crops can be grown. Since drain tiles increase productivity to this extent, they have been considered a good investment and installed widely. Bloss (1893, pg 9) describes tile drainage as the “only permanent improvements that you will ever put on your lands.”

Bloss (1893), Powers and Teeter (1916), Powers and Cretcher (1921) and Powers and King (1950) provide information for Willamette Valley drainage. Powers and Teeter (1916) provide the most complete technical manual for drainage installation. Powers and King (1950, pg 5-6) describe conditions where tile drains can be used to control the loss of water, soil, and plant food. They said this about drain tile effluent, “The water from a tile line is usually clear enough to wash in or even drink, while the run-off carries much plant food in suspension and in solution.”

$K_s$  is used in drainage equations to determine the appropriate spacing to install tile drains. However,  $K_s$  estimated from small-scale investigation may not reflect the tile system  $K_s$ . This can lead to installing tile drains that do not maximize economic efficiency. In some cases small-scale investigation may not be conducted, and tile drains are installed at some standard depth and spacing. If too many tile drains are installed water is flushed rapidly from the soil, which can cause high contaminant transport. If tile drains are installed too sparsely there may be a loss of crop yield. Understanding how small-scale  $K_s$  can be used in drainage design is important for efficient drainage to be installed.

## Literature Review

### **Hydraulic Conductivity**

Studies have shown that small-scale  $K_s$  laboratory and in-situ methods are extremely variable (Banton, 1993; Mirjat and Kanwar, 1994). Laboratory  $K_s$  measurements using cores showed the most variability. Oosterbaan and Hijland (1994) note that one advantage of large-scale  $K_s$  measurements is that they are less variable than small-scale measurements. This is attributed to the spatial integration of flow paths and natural irregularities in large-scale soil volume.

Mohanty et al. (1998) found a significant difference between  $K_s$  measured using different techniques for the same field sites. They attributed the difference to sample size, presence or absence of open-ended macropores, and measurement principles. It was found that  $K_s$  measurements of soil cores using the constant head permeameter method underestimated drain-tile flow. Measurements using the disc permeameter method performed best for predicting drain-flow and yielded the largest values for  $K_s$ . The other methods compared in this study are the Guelph permeameter, velocity permeameter, and double-tube permeameter.

A study by El-Mowelhi and van Schilfgaarde (1982) measured  $K_s$  using water table and flow measurements from tile drains, and found them to be somewhat larger than  $K_s$  measured using the auger hole method. This is the only study found that used drain tile data to measure  $K_s$ . However, given the breadth of the literature, it is likely that others have used this approach.

### **Contaminants in Tile Drains**

Kladivko et al. (2001) presents a review of studies regarding pesticide transport to tile drains. Tile drainage was found to decrease the overall export of pesticides to surface water by decreasing surface runoff. Pesticides sorb to soil particles and are transported with surface erosion from runoff. Soluble compounds such as nitrate nitrogen will travel to the tile drain more readily.

Southwick et al. (1997) compared drained versus undrained plots in regards to losses of metolachlor and trifluralin. Drainage reduced runoff volume by 24%, sediment losses in runoff by 75 %, metolachlor losses by 90% and trifluralin losses by 57%. The concentration of metolachlor in the first runoff event was eight times greater in the undrained fields as opposed to the drained fields. By the end of the season (180 days) 485 g/ha of metolachlor (21.7% of total applied) had been lost in the undrained fields in runoff as opposed to 50.3 g/ha (2.2% of total applied) for the drained fields. There were subsurface drainage losses, but this was limited to 0.62 g/ha (0.03% of total applied). This study shows that subsurface drainage reduces transport of pesticides to receiving water.

Pesticides are still a concern in tile lines; breakthrough times for these substances to appear in tile drains are shorter than conventionally thought. Breakthrough times range from 1 hour after precipitation for a chloride tracer (Laubel et al., 1999) to 6 days following an atrazine application (Rothstein et al., 1996). Sorokina et al. (1997) reports that 5 days after application and following 37 mm of rain, imazaquin concentration peaked at 20.1 µg/L. The rapid breakthrough times are attributed to preferential flow through macropores and indicate that the effective field-scale  $K_s$  is larger than  $K_s$ .

estimated from numerous small-scale point measurements. Haria et al. (1994) observed the onset of drain flow almost immediately with the onset of rainfall.

Madramootoo et al. (1992) looked at loss of N, P, and K in 5-ha tile-drained fields planted in potato. N concentrations ranged from 1.70 mg/L to 40.02 mg/L. P concentrations ranged from 0.002 mg/L to 0.052 mg/L. K concentrations were always less than 10 mg/L on one field, but mostly more than 10 mg/L on the other. Overall, the seasonal removal of N was 70 kg/ha on field 1 and 13.91 kg/ha on field 2. The seasonal P removal was less than 0.02 kg/ha for both fields. The potato is a shallow rooted crop; therefore nutrients are leached out of the root zone relatively quickly compared to deeper rooting crops. There was some increase in N and K concentrations following chemical fertilizer application. Scott et al. (1998) looked at soluble-P and fecal coliform concentration after a manure application. Contaminants were transported to the tile lines within one hour. 37% of the soluble-P applied was exported via the tile drains.

The objective of this study is to better understand the scale effect of measured  $K_s$  from core- to field-scales. In particular we seek to determine if permeability measured at the core scale provides an unbiased estimate of field-scale permeability as measured through field drainage by drain tiles. This will help determine if core measurements can be scaled for use in drainage design and management or large-scale modeling.

## Materials and Methods

### **Site Descriptions**

All field sites had tile-drains installed 4 ft deep, spaced 50 ft apart.

Field 1 was 30 acres planted in tall fescue. Dayton Silt Loam dominated the soil with sections of Concord Silt Loam (Langridge, 1987). Dayton Silt Loam is classified as *fine, smectitic, mesic Vertic Albaqualfs* (USDA-NRCS 04/2000b).

Concord Silt Loam is classified as *fine, smectitic, mesic Typic Endoaqualfs* (USDA-NRCS 04/2000a). These soils are poorly drained, slow runoff or ponding with very low permeability (USDA-NRCS 04/2000a, 04/2000b). Grass cultivation for seed or forage is very common in this soil series (Langridge, 1987). Dayton soils are also known as “whitelands” because of the bleached albic layer.

Field 2 was 30 acres planted in tall fescue. The soil was a mix of Dayton Silt Loam and Amity Silt Loam (Langridge, 1987). Amity Silt Loam is classified as *fine-silty, mixed, superactive, mesic Argiaquic Xeric Argialbolls* (USDA-NRCS 12/2001). Amity soil is somewhat poorly drained with slow runoff and moderately slow permeability (USDA-NRCS 12/2001).

Field 3 was a 2.9 acre separately drained section of a 23.4-acre field. The field was planted in sweet corn, spring 2000; Cayuse spring oats cover crop, fall 2000; sweet corn, spring 2001; tall fescue, fall 2001. The soil was approximately 80% Woodburn Silt Loam and 20% Amity Silt Loam (Otte et al. 1974). Woodburn Silt Loam is classified as *Fine-silty, mixed, superactive, mesic Aquultic Argixerolls* and is moderately well drained with slow to medium runoff and medium runoff (USDA-NRCS, 04/2001).

Field 4 was 2.9 acre separately drained section of a 24.9-acre field. The field was planted in perennial ryegrass. Field 4 was adjacent to field 3 and had the same soil characteristics as field 3.

### **Field Instrumentation**

Piezometers were installed in each field to observe water-table fluctuations along a perpendicular transect between two parallel tile-drains. The piezometers were 1.2-meter lengths of 2.71 cm outer diameter pipe with a 2.29 cm inner diameter. The bottom opening was covered with metal screen and cheesecloth to prevent soil intrusion. Rubber stoppers with copper U-tubes were placed in the top of the piezometer to prevent surface water intrusion while allowing transmitted air to maintain gauge pressure at the water table surface.

Vertical holes for piezometer installation were drilled using a 1.25 inch auger; lateral movement of the auger bit while drilling caused most holes to be about 1.5 inch in diameter. A soil slurry (thick mixture of soil and water) was worked into the hole with a rod of similar size of the piezometer to be installed. The piezometer was then placed in the hole, displacing slurry, and set flush with the soil surface. The slurry was necessary to fill the gap between the piezometer and soil. This prevented air gaps that would interfere with soil moisture measurements. The slurry also sealed the piezometer in the hole and prevented short-circuiting, caused by surface water flowing along the outside of the piezometer and filling the piezometer from the bottom.

11 piezometers were installed in field 1, spaced approximately 0, 3, 6, 11, 18, 25, 32, 39, 44, 47 and 50 feet from the tile drain. 16 piezometers were installed in field 2, starting at the tile drain the first three were spaced 2.5 feet apart, and the remaining 13

were spaced 5 feet apart. 20 piezometers were installed in field 3, all were spaced five feet apart. 21 piezometers were installed in field 4, all were spaced five feet apart.

Pressure sensors (In-Situ Mini-Troll; Standard Pressure, vented and non-vented; Professional, vented and non-vented; Laramie, WY) were rotated among the piezometers to measure water-table height in one-hour intervals. Water table height was also measured once a week by hand to verify the data.

Tipping bucket rain gauges (Davis Rain Collector II; Hayward, CA) with 0.2 mm readability were installed at each field site with event recording data loggers (Onset HOBO; Bourne, MA). The rain record was necessary to correlate water-table fluctuations with precipitation and identify suitable periods for analysis.

#### **Field-Scale $K_s$ Estimation**

Field-scale  $K_s$  was estimated using a classic solution to the time-dependent non-linear Boussinesq equation developed by Polubarinova-Kochina (P-K) (Polubarinova-Kochina, 1962) for the shape and evolution of a water-table draw down in response to parallel horizontal drains overlaying an impermeable layer. The P-K solution is:

$$h(x, t) = \frac{Hf\left(\frac{x}{l}\right)}{1 + 1.115 \frac{kHt}{mL^2}} \quad (1)$$

where:

$h(x, t)$  = the height of the water-table at position  $x$  and time  $t$

$H$  = the initial height of the water table

$f(x/l)$  = the function of the water-table height with respect to lateral displacement from drain. The function can be found in Polubarinova-Kochina (1962) pp. 515-516.

$k$  = the saturated hydraulic conductivity

$t$  = time

$m$  = the voidable porosity

$L$  = half the distance between drains

By dividing  $h(x,t_i)$  by  $h(x,t_0)$  this equation is made independent of  $x$  and we get:

$$\frac{h(x, t_i)}{h(x, t_0)} = \frac{1 + 1.115 \frac{kHt_0}{mL^2}}{1 + 1.115 \frac{kHt_i}{mL^2}} \quad (2)$$

where:

$h(x,t_0)$  = the initial water-table height at initial time  $t_0$

$h(x,t_i)$  = the water table height at subsequent time  $t_i$

The result of equation (2) will be referred to as  $h/h_0$  below

Predicted and measured values for  $h/h_0$  were compared using the error sum of squares.  $K_s$  was estimated by fitting a value to minimize the error sum of squares. When data from multiple piezometers was collected for the same event simultaneously  $K_s$  could be calculated using two methods. Method 1 assigned the same value of  $K_s$  to all of the piezometers. Method 2 assigned a unique value of  $K_s$  to each individual piezometer.

Both methods were used in this study.

Suitable events for field-scale  $K_s$  analysis were chosen that fit all of the following criteria: 1) Rainfall events where there is both a water table rise across the observed transect and the post-event water table height, measured from the tile drain, was at least twice the water table height previous to the event. 2) There is a crisp end of rainfall, defined as less than 1mm/day. 3) There is little intermediate rainfall that influenced the shape of the water table during the event.

### **Undisturbed Soil Core Sampling**

Undisturbed soil cores were taken in each field to characterize small-scale  $K_s$  and matric potential. For  $K_s$  analysis cores were collected in brass cylinders 5.4 cm in diameter and 6.0 cm in height ( $137.4 \text{ cm}^3$ ). For soil-moisture retention analysis cores were collected in brass cylinders 5.4 cm in diameter and 3.0 cm in height ( $68.7 \text{ cm}^3$ ). One core of each size was collected at depths of 30, 60, 90 and 120 cm at four sites in field 1 and field 2; and five sites in field 3 and field 4.

### **Small-Scale $K_s$ Estimation**

$K_s$  was estimated using a constant head permeameter (CHP) or falling head permeameter (FHP) as appropriate for the permeability presented. The CHP and FHP methods are described by Klute and Dirksen (1986). The CHP was used for a  $K_s$  range of  $2 \cdot 10^{-1} \text{ cm/s}$  to  $2 \cdot 10^{-6} \text{ cm/s}$  and the FHP was used for a  $K_s$  range of  $7 \cdot 10^{-4} \text{ cm/s}$  to  $10^{-10} \text{ cm/s}$ . The permeameter hydraulic conductivity was very large compared to the soil, and therefore was not subtracted from the soil  $K_s$ .

Soil cores were saturated by placing them vertically in a bath of 0.005 M  $\text{CaSO}_4$  solution with the fluid level just below the top of the core for 24 hours. The 0.005 M  $\text{CaSO}_4$  solution prevented dispersion of clays and maintained soil structure. Cores were then loaded in Tempe cells and placed in either a CHP or FHP.

The CHP employed a 1 liter mariotte bottle to supply water at a constant head. Piezometers immediately up- and down-stream of the Tempe cell were used to measure the change of head across the core on a meter-stick with 1 mm graduations. Water was collected over a known period of time into a graduated cylinder to measure flow.

The FHP used a 5ml burette with 0.01 ml graduations connected to the Tempe cell as the water source. Water height at the initial and finish time was measured on a meter-stick with 1mm graduations.

Darcy's law was used to calculate  $K_s$ . All cores collected were analyzed regardless of the presence of continuous vertical macropores, such as wormholes, that could cause pipe flow.

### **Soil-Moisture Retention Curves and Voidable Porosity**

68.7 cm<sup>3</sup> soil cores in brass rings were used to measure water retention according to methods described in Klute (1986). The bottom of the core was wrapped in cheesecloth and cores were saturated by placing vertically in a 0.005 M CaSO<sub>4</sub> solution for 24 hours with the fluid level just below the top of the cores. The cores were then put on saturated ceramic plates and placed in a pressure bomb until stabilized, determined by weighing the cores. When the cores stabilized the pressure was increased to the next step. Table 2 shows the pressures that the cores progressed in desorption for all four fields. Each sample site represented 4 cores, one from each sample depth. Voidable porosity, as employed in equation 2, was assumed to occur at a matric potential of -100 cmH<sub>2</sub>O (about 0.1 bar).

Table 2. Pressures used for soil-moisture retention curve. An "x" designates the samples were stabilized at the pressure.

Field	Site	Pressure (bar)								
		0.03	0.1	0.2	0.3	0.4	0.5	0.75	1	3
1	1	x	x	x	x	x	x	x	x	x
	2	x	x	x	x	x	x	x	x	
	3	x	x	x	x	x	x	x	x	x
	4	x	x	x	x	x	x	x	x	
2	1	x	x	x	x	x	x	x	x	x
	2	x	x	x	x	x	x	x	x	
	3	x	x	x	x	x	x	x	x	x
	4	x	x	x	x	x	x	x	x	
3	1	x	x				x		x	x
	2	x	x				x		x	x
	3	x	x	x	x	x	x	x	x	
	4	x	x	x	x	x	x	x	x	
	5	x	x		x		x		x	x
4	1	x	x				x		x	x
	2	x	x				x		x	x
	3	x	x				x		x	x
	4	x	x				x		x	x
	5	x	x		x		x		x	x

Once cores stabilized at the final pressure they were oven dried at 105°C for at least 24 hours. Dried soil was removed from the brass cylinder and weighed. The brass cylinder, cheesecloth, rubber band and label were weighed to subtract from the core weight recorded while in the pressure bomb. Brass cylinders that had the cheesecloth, rubber band and label, but no soil, were used as blanks to determine the cheesecloth water content (expressed in  $g_{H_2O}/g_{cheesecloth}$ ) at each pressure, which was subtracted from the core weight. These data were used to calculate water retention at the given matric potential, bulk density and voidable porosity.

## Results and Discussion

### Saturated Hydraulic Conductivity

Field-scale and small-scale  $K_s$  for fields 1, 2 and 4 are summarized in the following pages. The graphs include the arithmetic mean, geometric mean and harmonic mean as ways of characterizing the central tendency for the disparate values of small-scale  $K_s$ . The arithmetic mean is generally the largest estimate, and here was found to be in closest agreement with the field-scale  $K_s$  value. The arithmetic mean is dominated by the larger values, which is particularly influential when used to average over the 5-8 orders of magnitude range that small-scale  $K_s$  encompassed. Tables 3 summarizes small- and field-scale  $K_s$  using the arithmetic mean.

Table 3. Ratio of arithmetic mean small- and field-scale  $K_s$  (cm/s)

Field	Field-Scale $K_s$	Small-Scale $K_s$	Field-Scale $K_s$ / Small-Scale $K_s$
1	$5.5 \cdot 10^{-2}$	$4.7 \cdot 10^{-4}$	117.0
2	$7.8 \cdot 10^{-2}$	$3.4 \cdot 10^{-3}$	22.9
3	N/A	$2.7 \cdot 10^{-2}$	N/A
4	1.3	$2.1 \cdot 10^{-2}$	61.9

Table 4 shows the difference in variance between the small-scale measurements and field-scale measurements.

Table 4. Coefficient of Variance (COV) for small- and field-scale  $K_s$

Field	COV Field-Scale $K_s$	COV Small-Scale $K_s$
1	59.5%	224.5%
2	62.9%	193.1%
3	N/A	181.2%
4	48.5%	152.6%

All  $R^2$  values presented in the following figures represent the correlation between  $h/h_0$  predicted and  $h/h_0$  calculated. This provides an indicator of how well the model values fit the observed values.

### Field 1

Only one piezometer was usable for field-scale  $K_s$  estimation in field 1; therefore method 2 could not be used. Figure 1 shows the correlation of the piezometer response for all three events. A very good fit is displayed with  $R^2$  values of 0.97, 0.98, and 0.99 for the events. Event 1 followed a 30 mm precipitation event; over a 67-hour period from 03/06/2002 23h00 to 03/09/2002 18h00 the water table fell from 113 cm to 59 cm above the drain tile. Event 2 followed an 18 mm precipitation event; over a 274-hour period from 03/12/2002 13h00 to 03/23/2002 23h00 the water table fell from 112 cm to 47 cm above the drain tile. Event 3 followed a 12 mm precipitation event; over a 399-hour period from 03/24/2002 08h00 to 4/9/2002 11h00 the water table fell from 64 cm to 34 cm above the drain tile.

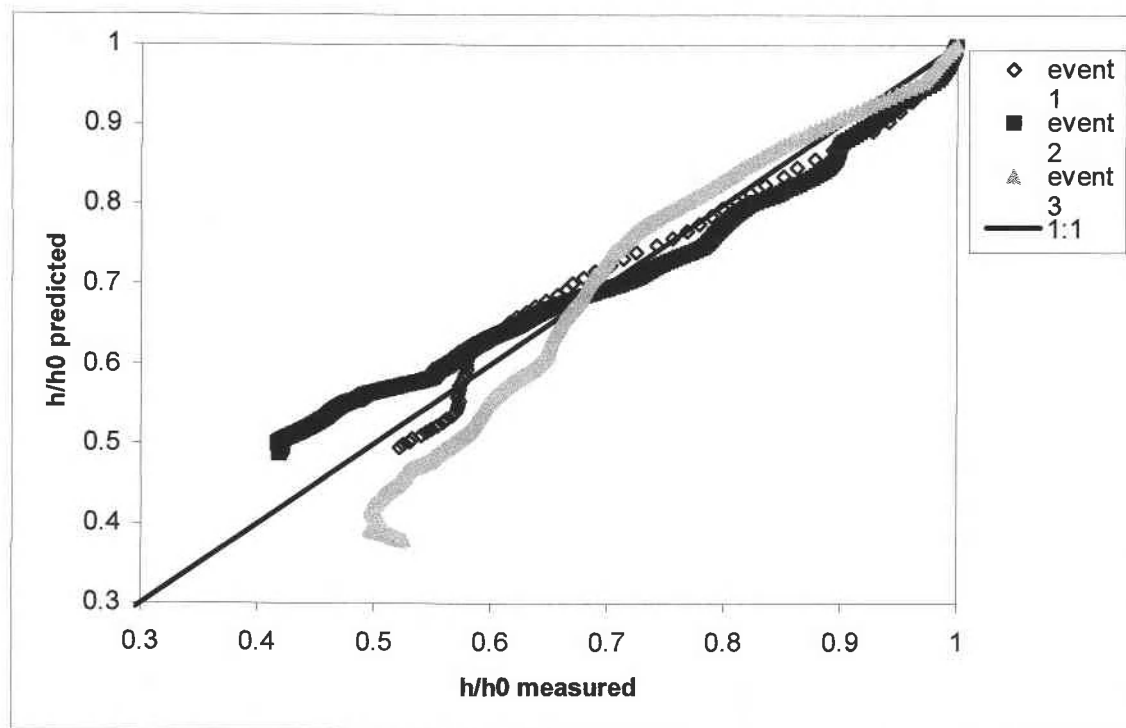


Figure 1. Correlation for field 1 in the 3 events analyzed. Only one piezometer was available for analysis during each event. Event 1  $R^2=0.97$ ; event 2  $R^2=0.98$ ; event 3  $R^2=0.99$

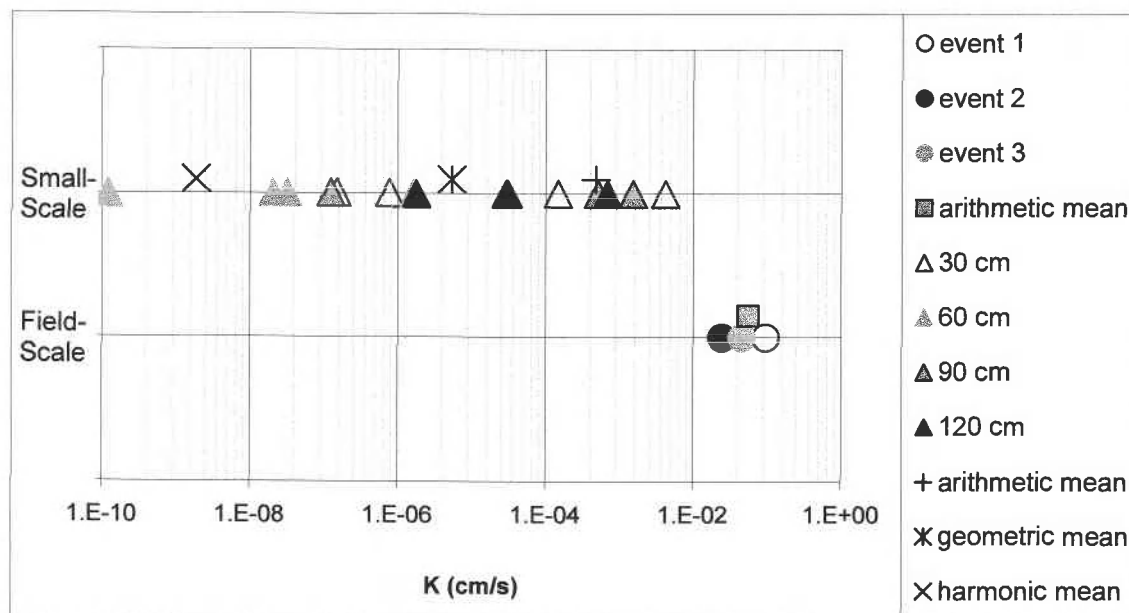


Figure 2. Field 1 comparison of field-scale  $K_s$  with small-scale  $K_s$ . Field-scale  $K_s$  was 117 times greater than small-scale  $K_s$  when comparing arithmetic means.

## Field 2

Field 2 had one suitable event for analysis. Method 1 gave a poor fit for piezometer 1 (see figure 3), which appeared to display lower  $K_s$ . However the resulting  $K_s$  value fell within the range of  $K_s$  values obtained using method 2, and provided a good estimate of overall  $K_s$ . The poor fit in method 1 was caused in large part from piezometer 1, if this piezometer was excluded from the analysis  $R^2 = 0.77$ . When method 2 was used the model fit was very good with an  $R^2$  value of 0.99 (see figure 4). Event 1 followed a 14 mm precipitation event. Over a 385-hour period from 03/27/2002 22h00 to 04/12/2002 23h00 the average water table height fell from 73 cm to 16 cm above the drain tile.

The model fit for event 1 in this field showed some curvature for both method 1 (see figure 3) and method 2 (see figure 4). In method 2 the curvature occurs when  $h/h_0$  is less than 0.4 and the water table height approached 0 cm. Similar curvature was also observed in field 4 event 3, under similar conditions, and is shown later. This was likely caused by an increased contribution of deep seepage to drainage when the water table height is low. The drains may not overlay an impermeable boundary. The model may not be applicable as the water table height approaches 0 cm.

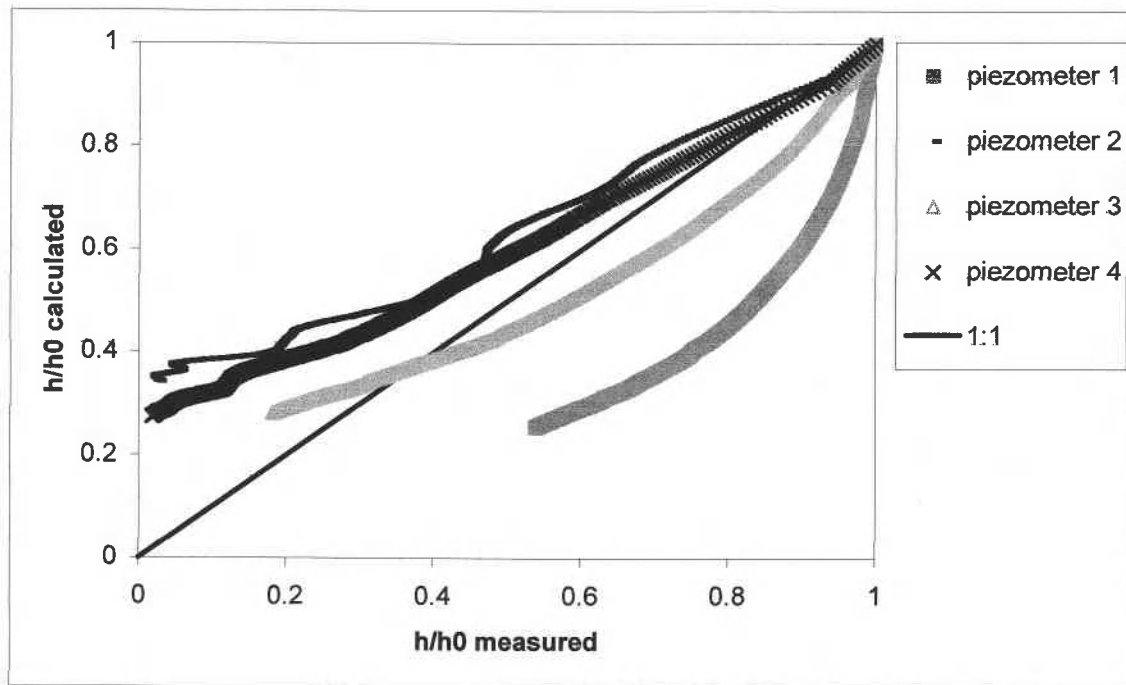


Figure 3. Correlation for field 2 event 1: method 1.  $R^2=0.39$

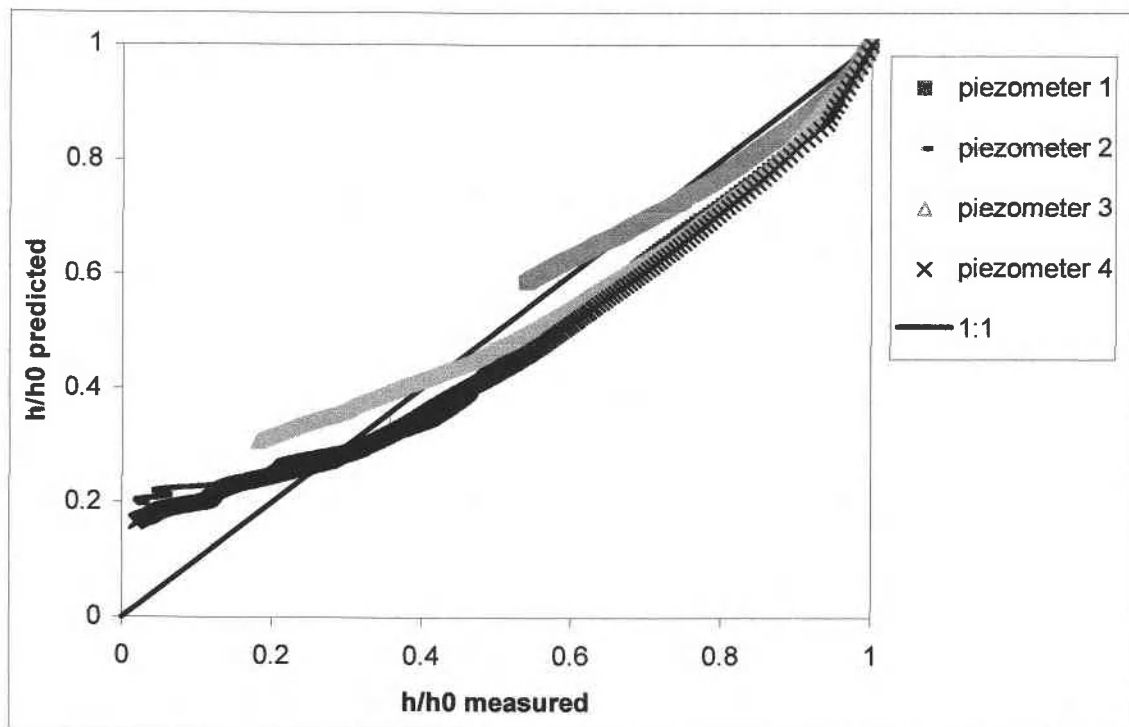


Figure 4. Correlation for field 2 event 1: method 2.  $R^2=0.99$

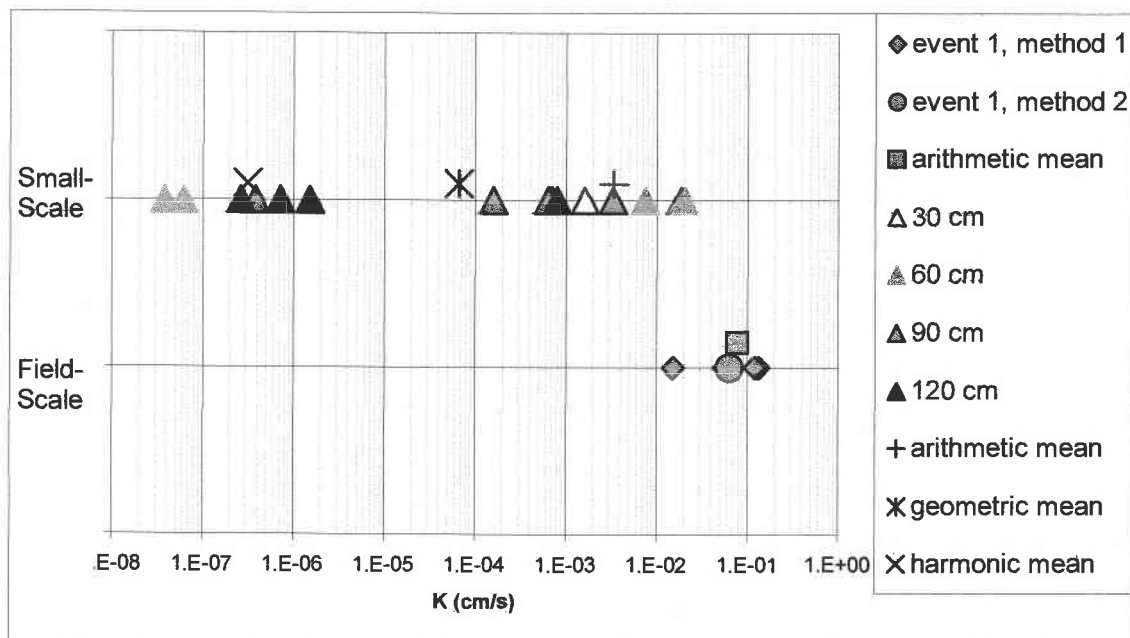


Figure 5. Field 2 comparison of field-scale  $K_s$  with small-scale  $K_s$ . Field-scale  $K_s$  was 23 times greater than small-scale  $K_s$  when comparing arithmetic means.

Field 2 had the least difference between small- and field-scale  $K_s$  of the fields.

The two greatest small-scale  $K_s$  values were greater than the lowest value of field-scale  $K_s$ ; however this value of field-scale  $K_s$  was from piezometer 1, which had the worst fit to the model (see figure 3)

### Field 3

There were no suitable events for field-scale  $K_s$  analysis in Field 3. Small-scale  $K_s$  is shown in figure 6.

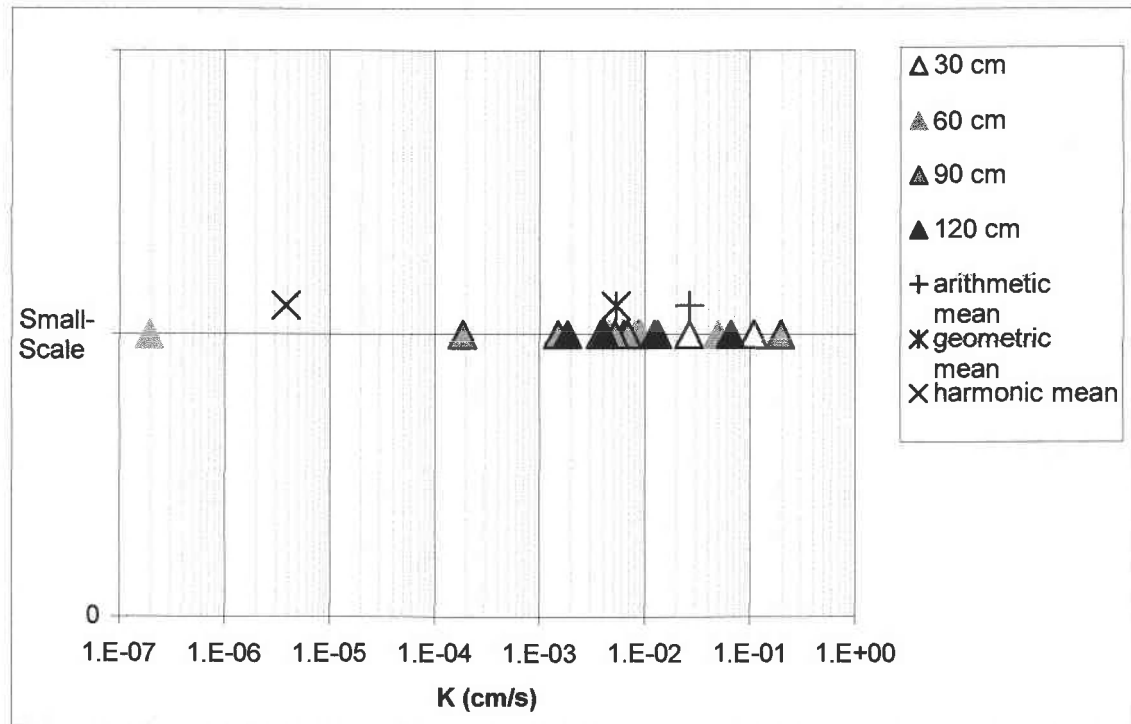


Figure 6. Field 3 small-scale  $K_s$

#### Field 4

There were 3 events in field 4 suitable for  $K_s$  estimation. Method 2 could be used with six piezometers in event 1 and four piezometers in events 2 and 3. Figures 7-12 show the model fit of methods 1 and 2 for each event. Method 2 provided a better fit than method 1 in each event. Event 1 followed a 24 mm precipitation event. Over a 64-hour period from 02/08/2002 07h00 to 02/10/2002 11h00 the average water table height fell from 31 cm to 7 cm above the drain tile. Event 2 followed a 25 mm precipitation event. Over an 88-hour period from 03/11/2002 20h00 to 03/15/2002 12h00 the average water table height fell from 35 cm to 7 cm above the drain tile. Event 3 followed an 18 mm precipitation event. Over a 70-hour period from 3/19/2002 13h00 to 3/22/2002 11h00 the average water table height fell from 19 cm to 2 cm above the drain tile.

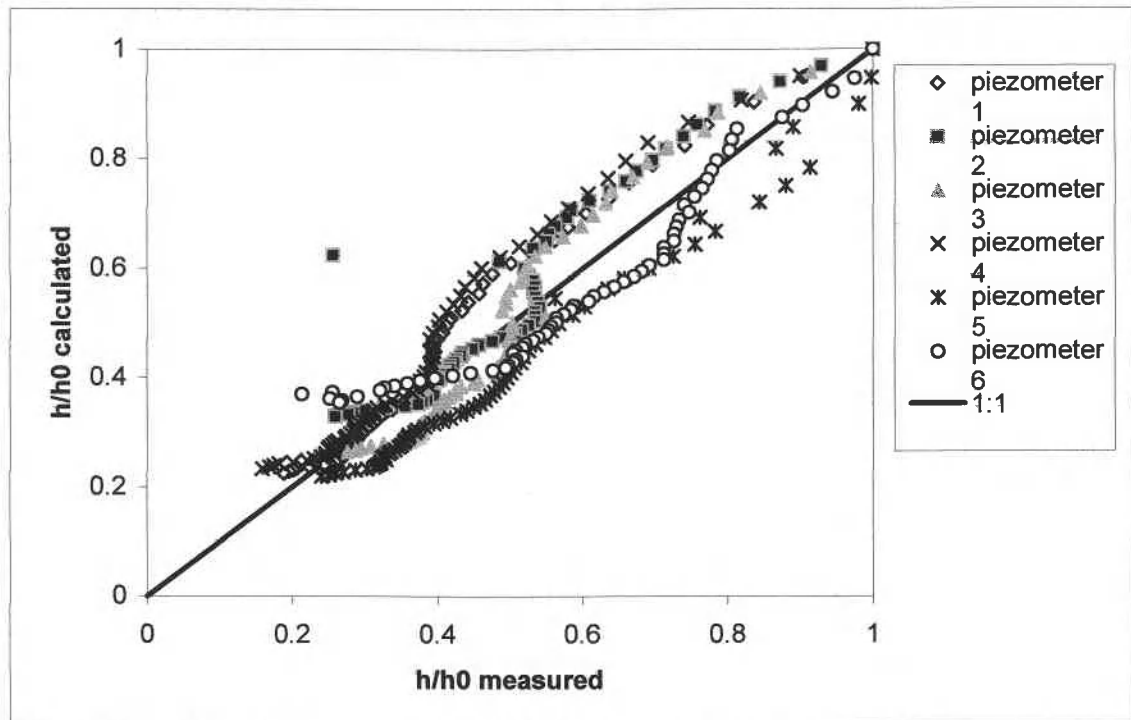


Figure 7. Correlation for field 4 event 1: method 1.  $R^2=0.92$

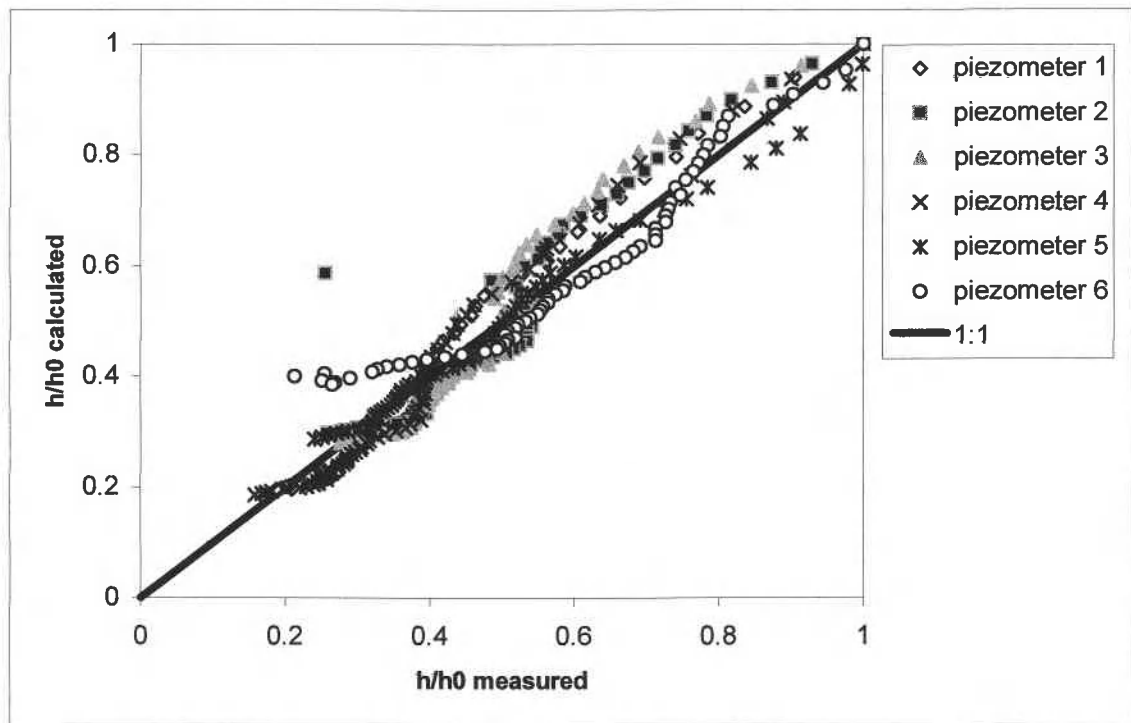


Figure 8. Correlation for field 4 event 1: method 2.  $R^2=0.95$

Event 2 showed a discrepancy between measured  $h/h_0$  values and those predicted by the model, highlighted in boxed regions of figures 9 and 10. The boxed regions show a change in  $h/h_0$  predicted, while  $h/h_0$  measured shows little change. This is possibly caused by an intermediate precipitation event that recharged the water table. A 4mm precipitation event lasting 5 hours started at hour 27 of the event.

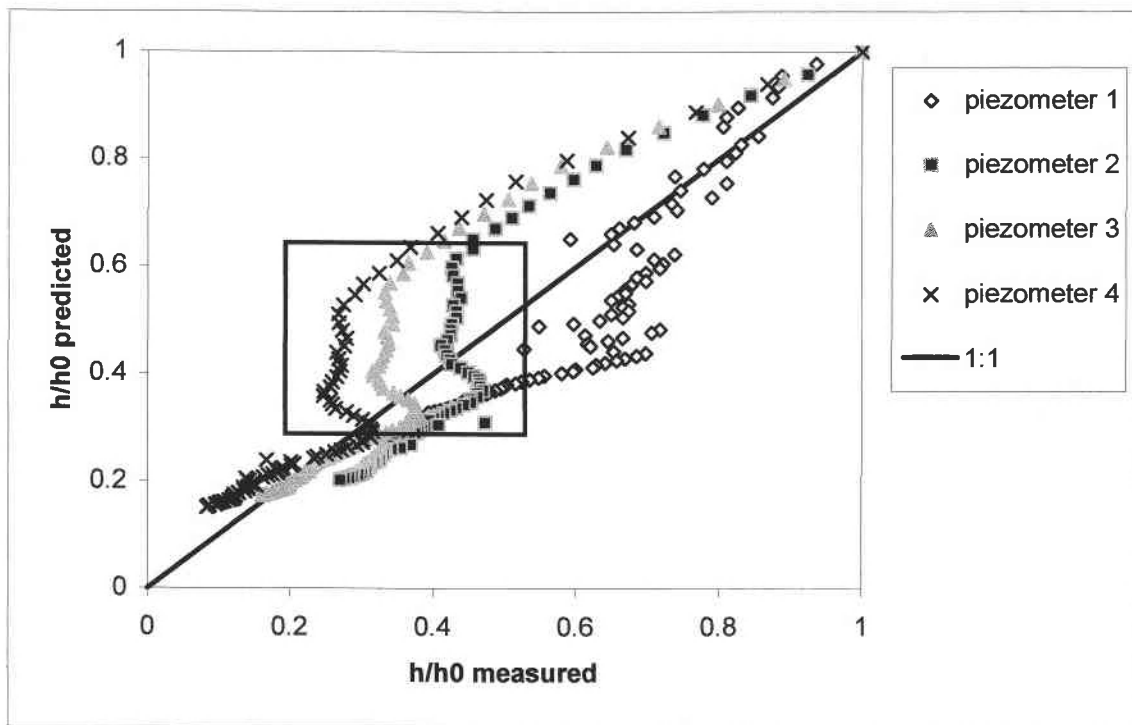


Figure 9. Correlation for Field 4 event 2: Method 1.  $R^2=0.73$ . The trend in the boxed area was caused by an intermediate rainfall event.

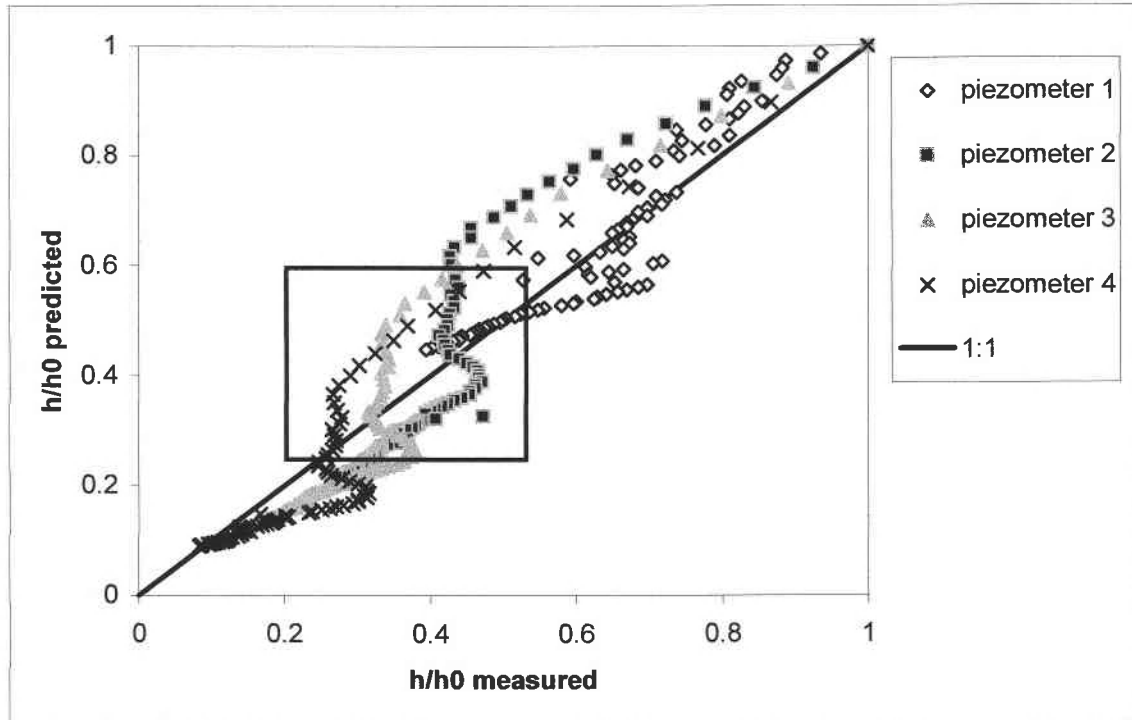


Figure 10. Correlation for field 4 event 2: method 2.  $R^2=0.90$ . The trend in the boxed area was caused by an intermediate rainfall event

Field 4 event 3 displays similar curvature in the model fit to the one seen in field 2 event 1. The water table approached 0 cm, likely resulting in deep seepage becoming a significant contributing factor to drainage. If deep seepage contributes to drainage the measured water table would draw down faster than predicted by the model. This is the characteristic shown by the curvature for this event.

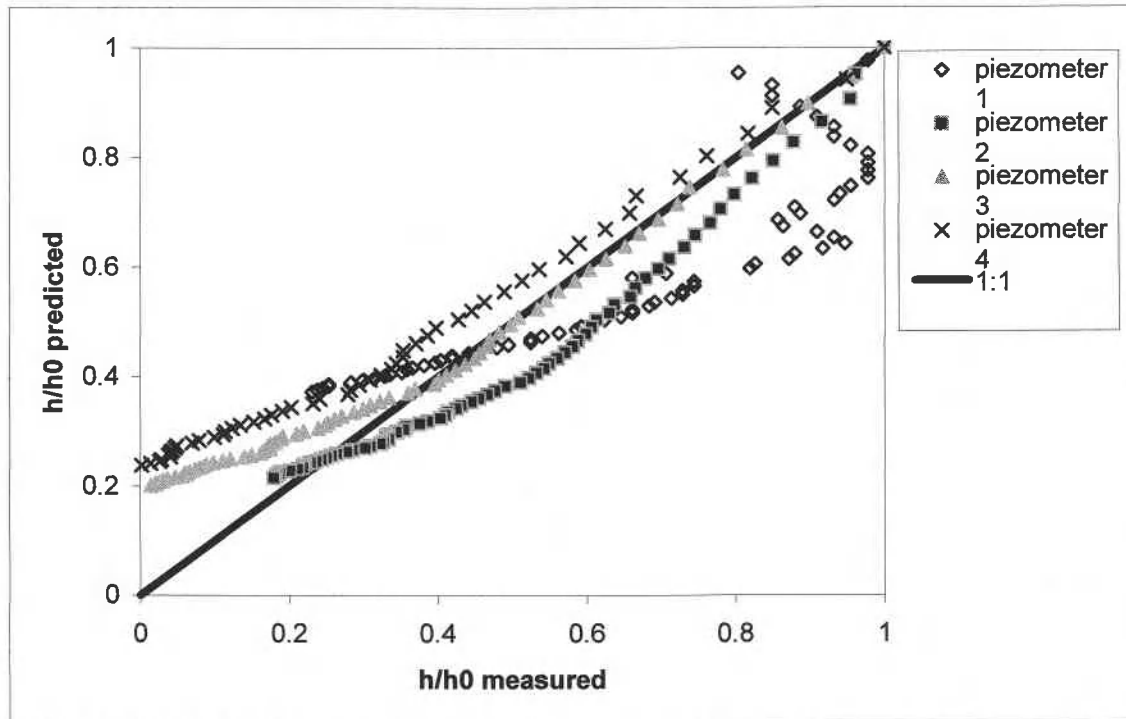


Figure 11. Correlation for field 4 event 3: method 1.  $R^2=0.87$

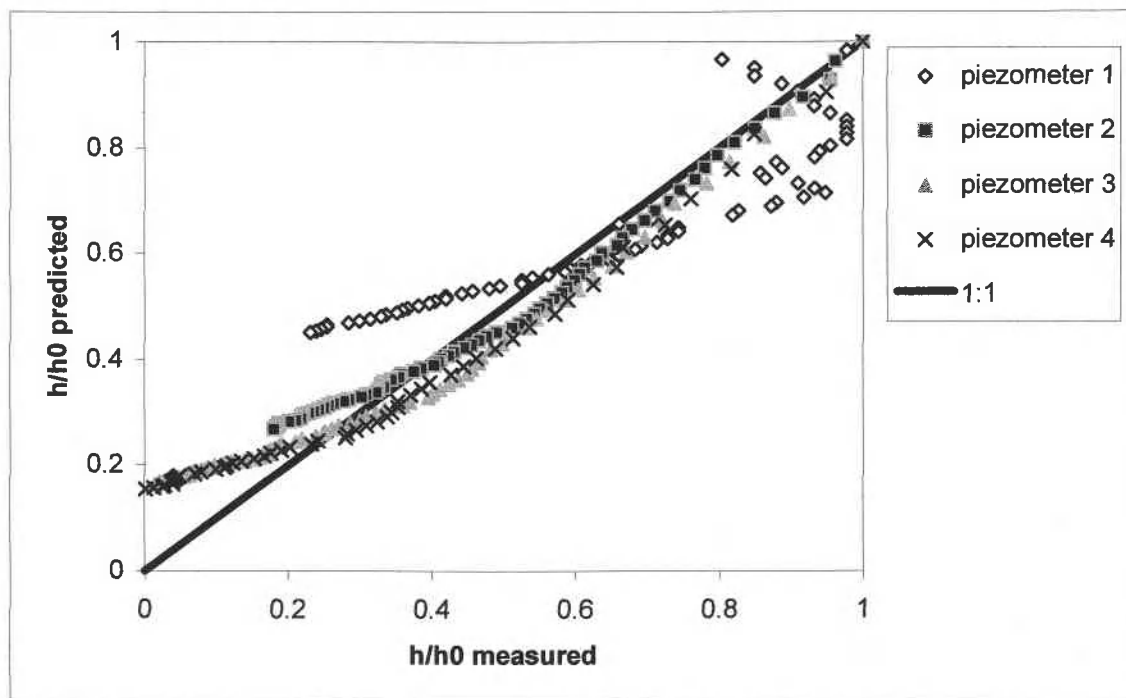


Figure 12. Correlation for field 4 event 3: method 2.  $R^2=0.93$

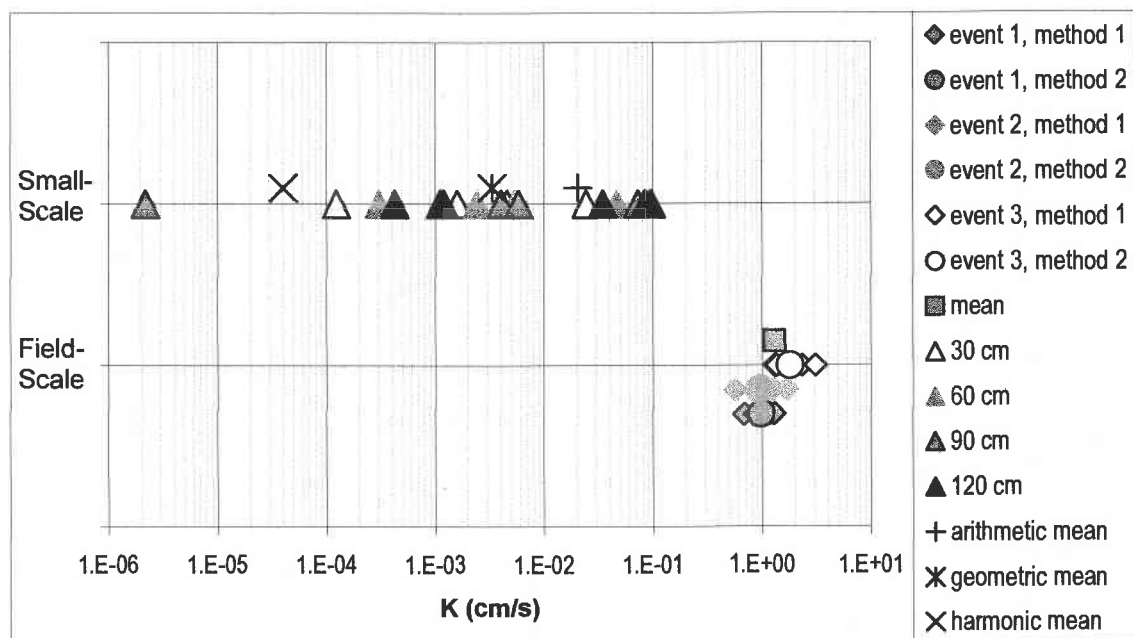


Figure 13. Field 4 comparison of field-scale  $K_s$  with small-scale  $K_s$ . Events are staggered vertically. Field-scale  $K_s$  was 62 times greater than small-scale  $K_s$  when comparing arithmetic means.

Field-scale  $K_s$  measurements were larger than the small-scale measurements by factors of 117, 23, and 62 when comparing the arithmetic means. Field Scale  $K_s$  also had much less variability than the small-scale  $K_s$ . Bouma et al. (1981) calculated that water-conducting voids occupy less than 2% of the total soil volume for heavy clay soil near the tile drain. Germann and Beven (1981) measured that macropores occupy 1% to 4.5% of the total soil volume. This indicates that large portions of small soil cores are not representative of the true hydrologic characteristics that determine transport. These samples would not contain water-conducting voids with consistent proportions between the samples, or with similar proportions to the field-scale soil media. Water-conducting voids within the core flow boundary would not have the same orientation as the transmitted water that exists in the field. These effects caused the measured values for  $K_s$  to be extremely variable. Other potential sources of error that can lead to variability

include core compaction, incomplete saturation, changes to soil structure during saturation, smearing, and restriction to flow by the apparatus. While these conditions ideally would not exist, they are common when using the standard laboratory method.

Using tile drains to measure  $K_s$  is inexpensive, effective and low maintenance if remote data loggers are used to measure water-table height and precipitation.

Disadvantages for using tile drains include: i) data can only be gathered during the rain season; ii) data accumulation requires significant time, on the order of months; iii) finding suitable events can be difficult because the water-table is very sensitive to intermediate precipitation; and iv) there is no standard method for the analysis of resulting data.

Using soil cores to measure  $K_s$  has the advantages that it can be done year round, and there is a standard sampling and testing protocol. However, collecting and testing a suitable number of cores is expensive and labor intensive; there is a high degree of spatial and temporal variability (Asare et al., 1993; Logsdon and Jaynes, 1996); and it is inaccurate if interested in field-scale processes.

Cores seemed to provide an indicator for comparison of  $K_s$  between fields. Table 5 shows that the ratio of  $K_s$  between fields was consistent for both the field- and small-scale  $K_s$  values by about a factor of 5.

Table 5. Comparison of  $K_s$  between fields.

$K_s$ ratio between fields	Field-scale $K_s$ ratio	Small-scale $K_s$ ratio
(Field 2 $K_s$ ) / (Field 1 $K_s$ )	1.42	7.2
(Field 4 $K_s$ ) / (Field 1 $K_s$ )	23.6	44.6
(Field 4 $K_s$ ) / (Field 2 $K_s$ )	16.67	6.17

Floyd (1958) used soil cores when investigating necessary drain spacing for three common soil series in the Willamette Valley. He found that soil series with smaller  $K_s$

values from core sampling required narrower drainage spacing, determined by observing water table height at midpoint between the tile drains, indicative of a smaller field-scale  $K_s$ .

Most precipitation in the Willamette Valley occurs during the winter months when there is little plant growth. There is low precipitation in the summer, typically not enough to raise the water table significantly during the growing season when plants are more susceptible to damage from water logging. Tile-drains in the Willamette Valley may not need to be designed based on rapid (days) water table draw-down to protect plants during the growing season, but on a gradual (weeks) water table draw-down that is sufficient to allow the fields to be worked earlier in spring. For perennial crops it is important to provide aerated soil conditions throughout winter, otherwise growth may be stunted and yield reduced.

The gradual draw down is displayed in fields 1 and 2 where the water table maintained a depth of about 30 cm during most of the winter and drew down to 100-120 cm depth over the course of three weeks in spring, as seen in figure 14

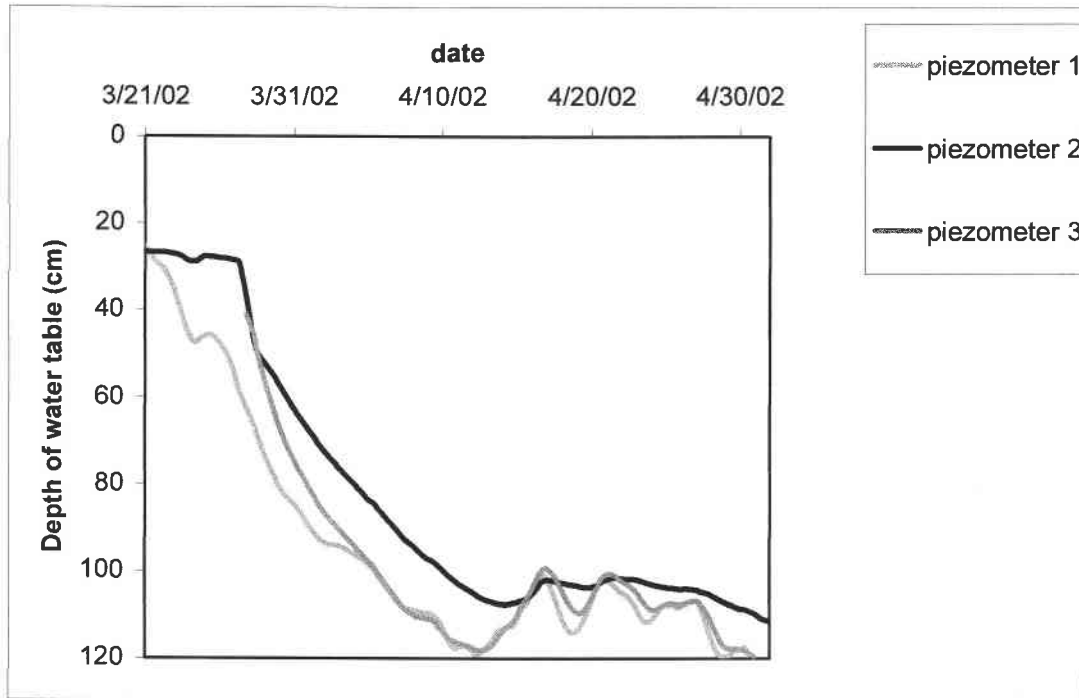


Figure 14. Spring water table draw down in field 2. Field 1 showed similar characteristics. The tile drains were at 120 cm depth.

Floyd (1958) recommended that tiles in Dayton soils (fields 1 and 2) be spaced at least 20 feet apart, however Powers and Cretcher (1921) recommended a tile spacing of 60 to 66 feet with a depth of 33 to 36 inches. Field 4 had very rapid draw down curves with the water table peaking above a 60 cm depth just twice during the winter and falling to 120 cm very rapidly over 4 to 5 days (see figure 15). The water table response was faster than necessary for crop growth, indicating the tile system was over designed for this portion of the field.

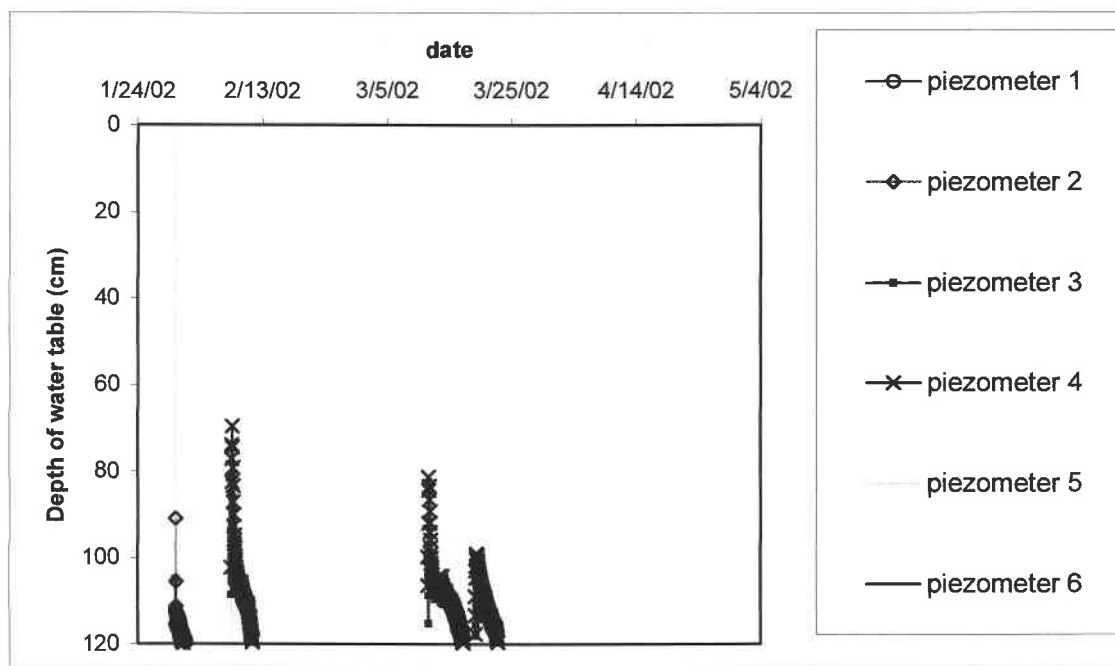


Figure 15. Water table draw down in field 4. The tile drains were at 120 cm depth.

### Matric Potential and Voidable Porosity

Voidable porosity is the fraction of the total soil volume that is voided under gravity drainage conditions. For this study, voidable porosity is defined as the difference in the air-filled soil volume fraction between saturation and water tension conditions of  $-100\text{cmH}_2\text{O}$  ( $\sim -10$  kPa). Figures 16-19 display the soil-moisture retention for each field in a water tension range of  $-3$  kPa to  $-30$  kPa. Tensions beyond this range were tested (up to  $-300$  kPa), but are not necessary in determining voidable porosity.

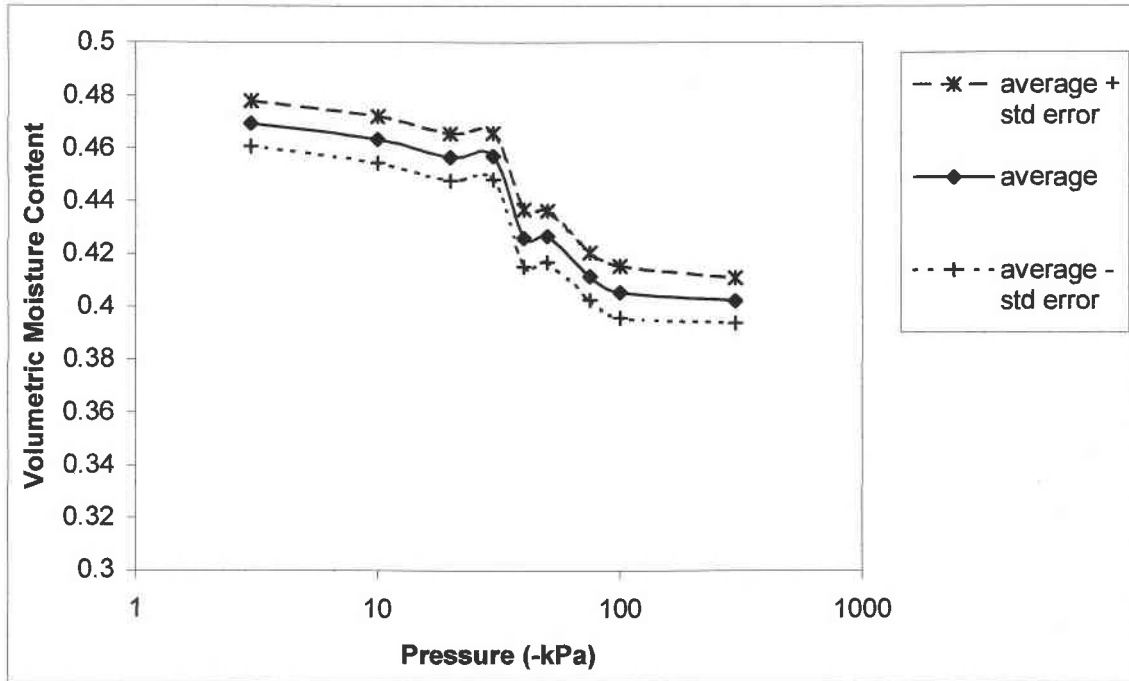


Figure 16. Field 1 soil-moisture retention from -3 kPa to -300 kPa

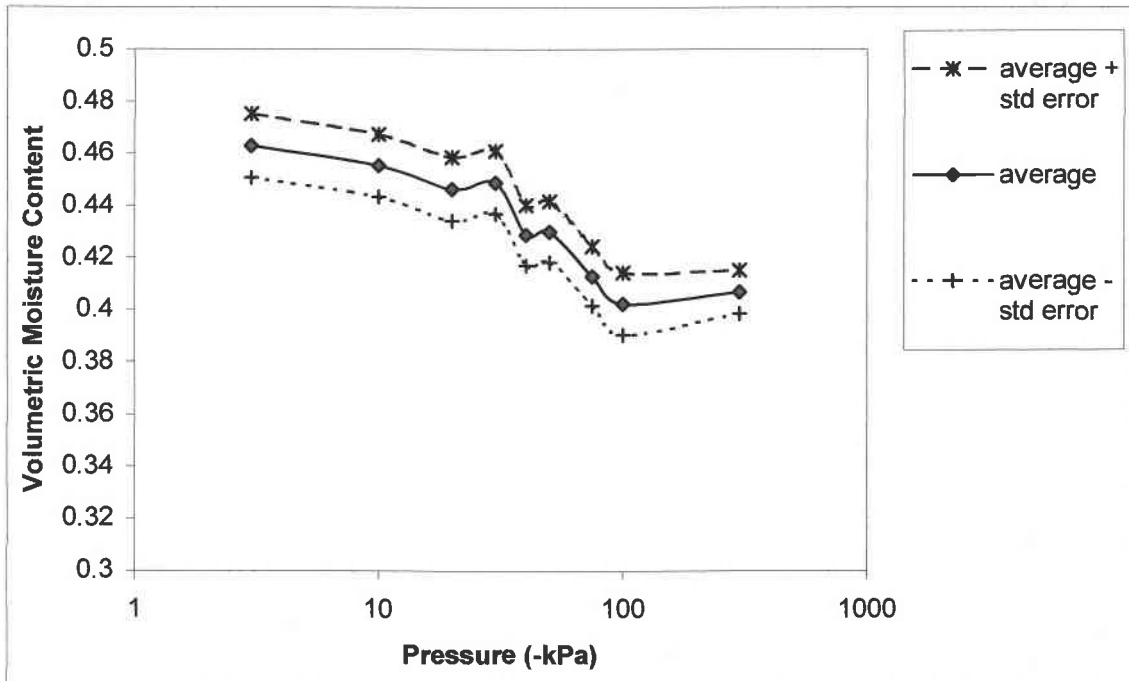


Figure 17. Field 2 soil-moisture retention -3 kPa to -300 kPa

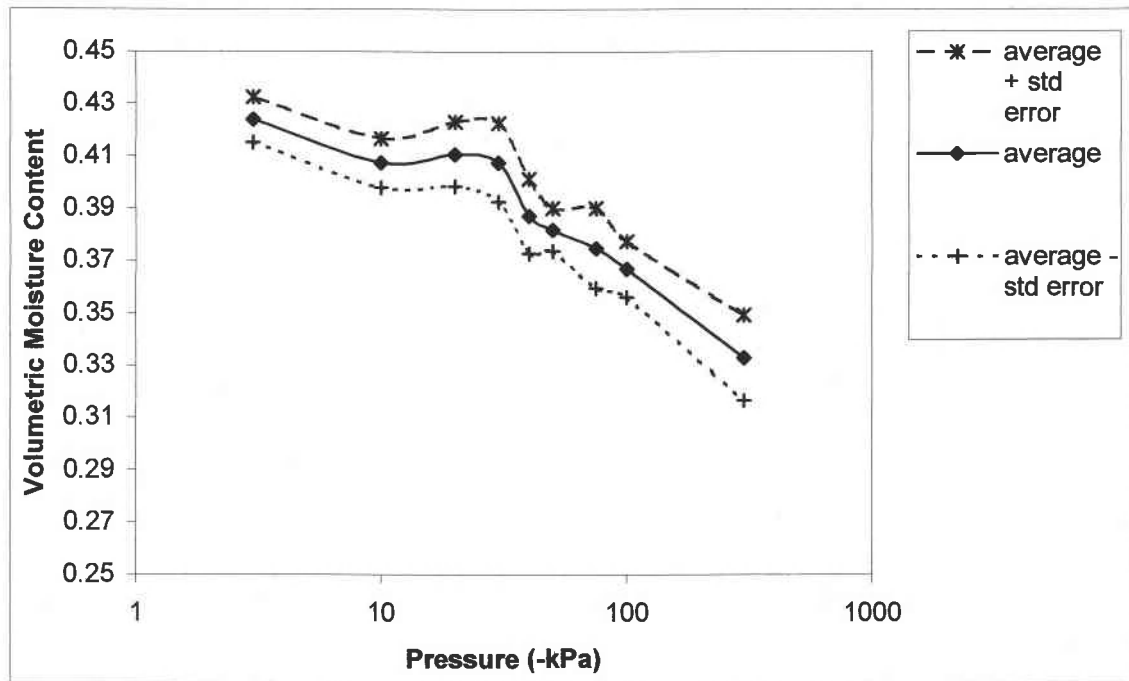


Figure 18. Field 3 soil-moisture retention from  $-3$  kPa to  $-300$  kPa

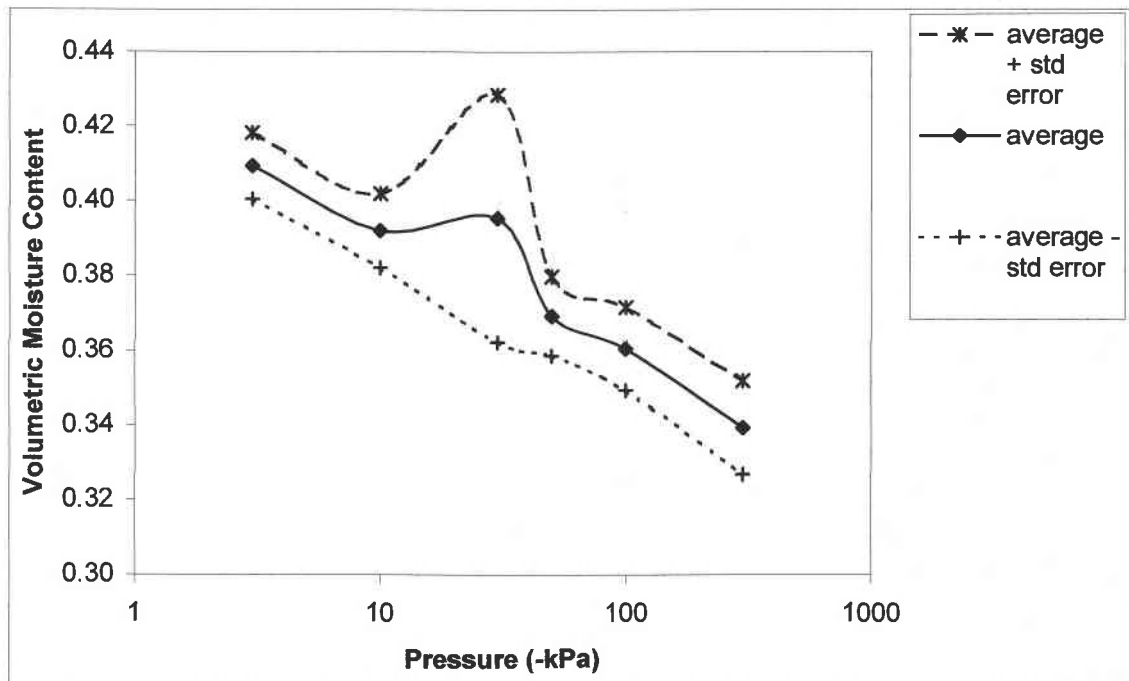


Figure 19. Field 4 soil-moisture retention from  $-3$  kPa to  $-300$  kPa

Unfortunately an accurate measurement of volumetric water content at saturation (tension of 0 kPa) is difficult to obtain and the water content differences between

saturation and  $-3$  kPa are unknown. The saturated water content can be estimated to equal the porosity. To compute this we assumed that 1) particle density was equal to  $2.65$  g/cm<sup>3</sup> and 2) At saturation all pores were completely filled with water without entrapped air voids. Assumption 1 is standard when performing soil physical analysis. Assumption 2 is very difficult to achieve in either laboratory or field conditions where there is typically some entrapped air in the soil cores that cause porosity to over-estimate saturated water content.

The fields displayed a moisture content change of about 2% between  $-3$  kPa and  $-10$  kPa. Therefore 2% represents a minimum value of voidable porosity. It then becomes necessary to estimate the change of moisture content between saturation and  $-3$  kPa. If the soil-moisture retention curves are extrapolated to 0 kPa there appears to be about a 5% change in moisture content between 0 kPa and  $-10$  kPa. For this reason a value of 0.05 was chosen to represent the voidable porosity. This estimate is subject to uncertainty without further data.

Despite the uncertainty in voidable porosity the model fit will not be affected if a different voidable porosity is used.  $K_s$  and voidable porosity are directly proportional ( $K_s/m = \text{constant}$ ) in equation (1). The water volume that must be transmitted over a constant time period increases as voidable porosity increases, requiring an increased  $K_s$ . If a more suitable voidable porosity value is determined  $K_s$  can easily be adjusted.

### **Bulk Density**

Bulk density was measured on the same cores that were used for the soil-moisture retention curve. Figure 20 summarizes the results for all fields. Bulk density decreased

with depth in all fields, most likely due to soil compaction from heavy agricultural equipment.

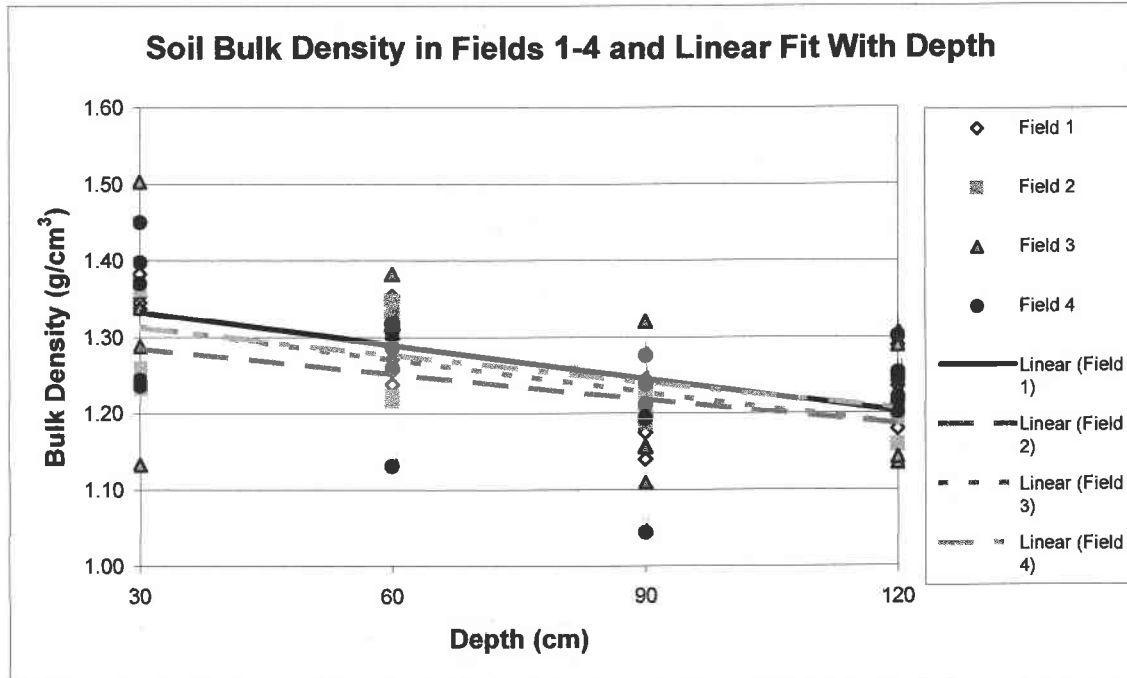


Figure 20. Soil bulk density for all fields based on depth.

## Conclusions

Saturated hydraulic conductivity ( $K_s$ ) was measured at four field sites using constant head and falling head permeameters on undisturbed soil cores and the Polubarinova-Kochina (P-K) solution for water table draw down between two parallel drains. Soil-moisture retention was also measured to determine voidable porosity.

$K_s$  measurements using undisturbed soil cores are a small-scale measurement ( $\sim 150\text{cm}^3$ ) and displayed a coefficient of variance (COV) of 150% to 225% within the same field and soil layers. These measurements are of low utility. With an objective of obtaining an overall  $K_s$  value that will reflect the true operational flow processes, use of the P-K solution is a field-scale procedure and displays a good fit between measured and calculated values of  $h/h_0$ .  $K_s$  values measured using this solution were greater by a factor of 23 to 117 and displayed a COV of only 50% to 60%, much less than the core measurements. This can be attributed to the spatial integration of macropores, flow irregularities and flow direction that tile-drains provide over a much larger sample volume ( $>100\text{m}^3$ ), encompassing all of the operational flow processes. There are also errors in measuring small-scale  $K_s$  as a result of the standard laboratory methods that lead to increased variability

Using the arithmetic mean to characterize the wide range (5-8 orders of magnitude) of small-scale  $K_s$  values compares to field-scale measurements that are 23 to 117 times greater. Under these conditions the arithmetic mean is dominated by the greatest values, similar to water-conducting voids which have a high water conductivity, but make up very little of the soil volume. Representing the small-scale  $K_s$  values with

the geometric and harmonic means increases this discrepancy by one to five orders of magnitude.

The high  $K_s$  values for field-scale measurements indicate rapid transport of water, if there is a free flowing outlet, and therefore potentially rapid contaminant transport from the soil surface to the tile drains. Rapid transport should be expected under the agricultural tile drain conditions described here. Higher than expected  $K_s$  also indicates that tile drain installation spacing may be narrower than necessary, as is possibly the case in field 4. A wider spacing might provide adequate drainage at less cost.

The method used to measuring field-scale  $K_s$  in this study is inexpensive, simple, effective and easily used where tile drains have been installed. All that is required is a piezometer to observe water table fluctuations and a rain gauge. One piezometer is adequate as demonstrated in field 1, although multiple piezometers and data with at least an hourly resolution was preferred. This method does not require flow meters that can be cumbersome to install and maintain; and eliminates the need to know total tile length, which can be difficult to survey in some field sites.

### References

- Asare, S.N.; Rudra, R.P.; Dickinson, W.T.; and Wall, G.J. (1993). "*Seasonal Variability of Hydraulic Conductivity.*" Transactions of the ASAE., 36(2):451-457
- Banton, O. (1993). "*Field- and Laboratory-Determined Hydraulic Conductivities Considering Anisotropy and Core Surface Area.*" Soil Science Society of America Journal. 57:10-15
- Bloss, J.M. (1893). "*Drainage.*" Oregon Agricultural Experiment Station. Bulletin 26
- El-Mowelhi, N.M. and van Schilfgaarde, J. (1982). "*Computation of Soil Hydrological Constants from Field Drainage in Some Soils of Egypt.*" Transactions of the ASAE 25:984-986
- Floyd, R.T. Jr. (1958). "*Drainage Studies on Dayton, Amity, and Willamette Soils in the Willamette Valley, Oregon.*" Oregon State College. 75 p.
- Haria, A.H.; Johnson, A.C.; Bell, J.P.; and Batchelor, C.H. (1994). "*Water Movement and Isoproturon Behaviour in a Drained Heavy Clay Soil: 1 Preferential flow Process.*" Journal of Hydrology. 163:203-216
- Germann, P. and Beven, K. (1981). "*Water Flow in Soil Macropores I. An Experimental Approach.*" Journal of Soil Science. 32:1-13
- Kladivko, E.J.; Brown, L.C.; and Baker, J.L. (2001). "*Pesticide Transport to Subsurface Tile Drains in Humid Regions of North America.*" Critical Reviews in Environmental Science and Technology. 31(1):1-62
- Klute, A. (1986). "*Water Retention: Laboratory Methods.*" Methods of Soil Analysis, Part 1. Agronomy Monograph No 9, 2<sup>nd</sup> Ed. 635-662.
- Klute, A. and Dirksen, C. (1986). "*Hydraulic Conductivity and Diffusivity: Laboratory Methods.*" Methods of Soil Analysis, Part 1. Agronomy Monograph No 9, 2<sup>nd</sup> Ed. 687-734
- Langridge, R.W. (1987). "*Soil Survey of Linn County Area, Oregon.*" USDA – Soil Conservation Service. Washington D.C.
- Laubel, A.; Jacobsen, O.H.; Kronvang, B.; Grant, R.; and Anderson, H.E. (1999). "*Subsurface Drainage Loss of Particles and Phosphorous from Field Plot Experiments and a Tile-Drained Catchment.*" Journal of Environmental Quality. 28:576-584

- Logsdon, S.D. and Jaynes, D.B. (1996). "*Spatial Variability of Hydraulic Conductivity in a Cultivated Field at Different Times.*" Soil Science Society of America Journal. 60:703-709
- Madramootoo, C.A.; Wiyo, K.A.; and Enright, P. (1992). "*Nutrient Losses Through Tile Drains from Two Potato Fields.*" Applied Engineering In Agriculture. 8(5):639-646
- Mirjat, M.S. and Kanwar, R.S. (1994). "*A Comparison of Two Saturated Hydraulic Conductivity Measuring Techniques in Relation to Drain Installation Methods.*" Applied Engineering in Agriculture. 10(1):65-68
- Mohanty, B.P.; Skaggs, T.H.; and van Genuchten, M.Th. (1998). "*Impact of Saturated Hydraulic Conductivity on the Prediction of Tile Flow.*" Soil Science Society of America Journal. 62:1522-1529
- Oosterbaan, R.J. and Nijland H.J. (1994). "*Determining the Saturated Hydraulic Conductivity.*" Drainage Principles and Application, Ed. Ritzema, H.P., International Institute for Land Reclamation and Improvement No. 16, 2<sup>nd</sup> ed. 435-476
- Otte, E.G.; Setness, D.K.; Walter, A.A.; Herbert, F.J. Jr.; and Knezevich, C.A. (1974). "*Soil Survey of the Yamhill Area, Oregon.*" USDA – Soil Conservation Service., Washington D.C.
- Polubarinova-Kochina, P.Y. (1962). "*Theory of Groundwater Movement.*" Translator: De Weist, R.J. Princeton University Press. 613 p.
- Powers, W.L.; and Cretcher, W. (1921) "*Farm Drainage.*" Oregon Agricultural College Experiment Station. Station Bulletin 178
- Powers, W.L., and King, A.S. (1950). "*Drainage Practices for Oregon.*" Oregon Agricultural Experiment Station. Station Bulletin 492
- Powers, W.L., and Teeter, T.A.H. (1916). "*The Drainage of "White Land" and Other Wet Lands in Oregon.*" Oregon Agricultural College Experiment Station. Station Bulletin 137
- Rothstein, E.; Steenhuis, T.S.; Peverly, J.H., and Geohring, L.D. (1996). "*Atrazine Fate on a Tile Drained Field in Northern New York: A Case Study.*" Agricultural Water Management. 31:195-203
- Scott, C.A; Geohring, L.D.; and Walter, M.F. (1998). "*Water Quality Impacts of Tile Drains in Shallow, Sloping, Structured Soils as Affected by Manure Application.*" Applied Engineering in Agriculture. 14(6):599-603

- Shipitalo, M.J. and Gibbs, F. (2000). "*Potential of Earthworm Burrows to Transmit Animal Wastes to Tile Drains.*" Soil Science Society of America Journal. 64:2103-2109
- Sorokino, M.N. and Thomas, G.W. (1997). "*Imazaquin Leaching in Karnak Soil in Kentucky.*" Weed Science. 45:722-726
- Southwick, L.M.; Willis, G.H.; Mercado, O.A.; and Bengtson, R.L. (1997). "*Effect of Subsurface Drains on Runoff Losses of Metalochlor and Trifluralin from Mississippi River Alluvial Soil.*" Archives of Environmental Contamination and Toxicology. 32:106-109
- USDA-NRCS. (12/2001). "*Official Series Description - AMITY Series -*"  
<<http://ortho.ftw.nrcs.usda.gov/cgi-bin/osd/osdname.cgi?-P>> Accessed November 21, 2002
- USDA-NRCS. (04/2000b). "*Official Series Description - DAYTON Series -*"  
<<http://ortho.ftw.nrcs.usda.gov/cgi-bin/osd/osdname.cgi?-P>> Accessed November 21, 2002
- USDA-NRCS. (04/2000a). "*Official Series Description - CONCORD Series -*"  
<<http://ortho.ftw.nrcs.usda.gov/cgi-bin/osd/osdname.cgi?-P>> Accessed November 21, 2002
- USDA-NRCS. (04/2001). "*Official Series Description - WOODBURN Series -*"  
<<http://ortho.ftw.nrcs.usda.gov/cgi-bin/osd/osdname.cgi?-P>> Accessed November 21, 2002
- Warren, K.L.; Rupp, D.E.; Selker, J.S.; Dragila, M.I.; and Peachy, R.E. (2002). "*Nitrate and Pesticide Transport From Tile-Drained Fields in the Willamette Valley, Oregon.*" presented at American Geophysical Union Fall 2002 Meeting, San Francisco, CA. 12/06/2002 – 12/10/2002.

**Appendix A: Soil-moisture Retention Data**

Table 6. Field 1 desorption soil-moisture retention data. Values are volumetric water content.

	Pressure (kPa)								
	3.296	10.006	19.995	29.992	39.990	49.987	74.463	99.974	296.476
Site1-30cm	0.430	0.428	0.425	0.425	0.377	0.383	0.375	0.366	0.375
Site1-60cm	0.482	0.474	0.473	0.473	0.463	0.464	0.443	0.444	0.420
Site1-90cm	0.486	0.477	0.476	0.480	0.433	0.414	0.414	0.410	0.402
Site1-120cm	0.455	0.455	0.448	0.448	0.410	0.428	0.417	0.404	0.404
Site2-30cm	0.391	0.378	0.368	0.374	0.346	0.349	0.336	0.327	
Site2-60cm	0.507	0.505	0.495	0.496	0.477	0.477	0.442	0.436	
Site2-90cm	0.515	0.509	0.504	0.505	0.493	0.474	0.463	0.449	
Site2-120cm	0.481	0.472	0.465	0.460	0.433	0.436	0.427	0.422	
Site3-30cm	0.466	0.464	0.457	0.459	0.412	0.419	0.403	0.402	0.396
Site3-60cm	0.510	0.505	0.497	0.498	0.474	0.471	0.450	0.464	0.451
Site3-90cm	0.463	0.457	0.447	0.447	0.423	0.431	0.414	0.403	0.393
Site3-120cm	0.470	0.462	0.453	0.449	0.437	0.428	0.416	0.398	0.377
Site4-30cm	0.427	0.422	0.413	0.416	0.349	0.357	0.345	0.339	
Site4-60cm	0.491	0.485	0.478	0.478	0.416	0.427	0.415	0.418	
Site4-90cm	0.500	0.492	0.484	0.482	0.468	0.465	0.440	0.438	
Site4-120cm	0.437	0.431	0.425	0.422	0.403	0.403	0.382	0.369	

Table 7. Field 2 desorption soil-moisture retention data. Values are volumetric water content.

	Pressure (kPa)								
	3.296	10.006	19.995	29.992	39.990	49.987	74.463	99.974	296.476
Site 1-30cm	0.508	0.503	0.499	0.501	0.494	0.488	0.477	0.466	0.450
Site 1-60cm	0.499	0.493	0.474	0.482	0.446	0.446	0.423	0.416	0.427
Site 1-90cm	0.501	0.482	0.482	0.485	0.427	0.458	0.438	0.419	0.406
Site 1-120cm	0.471	0.463	0.458	0.458	0.430	0.440	0.420	0.417	0.405
Site 2-30cm	0.358	0.347	0.335	0.337	0.324	0.323	0.309	0.293	
Site 2-60cm	0.444	0.438	0.428	0.426	0.414	0.405	0.398	0.354	
Site 2-90cm	0.516	0.499	0.493	0.493	0.485	0.480	0.459	0.463	
Site 2-120cm	0.498	0.489	0.483	0.482	0.471	0.468	0.451	0.432	
Site 3-30cm	0.456	0.455	0.448	0.447	0.437	0.438	0.425	0.419	0.413
Site 3-60cm	0.448	0.444	0.431	0.438	0.420	0.424	0.400	0.400	0.385
Site 3-90cm	0.425	0.423	0.401	0.418	0.410	0.408	0.393	0.386	0.382
Site 3-120cm	0.452	0.433	0.431	0.433	0.419	0.420	0.414	0.408	0.387
Site 4-30cm	0.487	0.484	0.476	0.477	0.425	0.422	0.404	0.400	
Site 4-60cm	0.356	0.356	0.349	0.349	0.337	0.333	0.315	0.307	
Site 4-90cm	0.490	0.485	0.473	0.473	0.449	0.455	0.431	0.422	
Site 4-120cm	0.500	0.492	0.480	0.482	0.473	0.472	0.449	0.433	

Table 8. Field 3 desorption soil-moisture retention data. Values are volumetric water content.

	Pressure (kPa)								
	3.103	3.296	9.810	10.006	10.342	19.995	29.992	30.682	39.990
Site 1-30cm	0.388				0.373				
Site 1-60cm	0.383				0.365				
Site 1-90cm	0.417				0.395				
Site 1-120cm	0.428				0.399				
Site 2-30cm	0.400				0.374				
Site 2-60cm	0.465				0.438				
Site 2-90cm	0.426				0.400				
Site 2-120cm	0.440				0.419				
Site 3-30cm	0.000	0.390		0.369		0.366	0.366		0.349
Site 3-60cm	0.000	0.452		0.448		0.444	0.446		0.408
Site 3-90cm	0.000	0.428		0.420		0.417	0.420		0.405
Site 3-120cm	0.000	0.458		0.441		0.437	0.436		0.395
Site 4-30cm	0.000	0.386		0.365		0.355	0.361		0.350
Site 4-60cm	0.000	0.475		0.460		0.449	0.452		0.421
Site 4-90cm	0.000	0.412		0.404		0.400	0.401		0.386
Site 4-120cm	0.000	0.431		0.426		0.417	0.422		0.407
Site 5-30cm	0.317		0.296					0.274	
Site 5-60cm	0.483		0.475					0.461	
Site 5-90cm	0.451		0.446					0.433	
Site 5-120cm	0.445		0.433					0.416	

Table 8 cont.

	49.987	51.366	74.463	99.974	293.029	296.476
Site 1-30cm		0.338		0.330	0.298	
Site 1-60cm		0.339		0.333	0.313	
Site 1-90cm		0.363		0.350	0.317	
Site 1-120cm		0.387		0.390	0.376	
Site 2-30cm		0.343		0.338	0.318	
Site 2-60cm		0.420		0.424	0.394	
Site 2-90cm		0.387		0.387	0.371	
Site 2-120cm		0.402		0.397	0.380	
Site 3-30cm	0.341		0.287	0.281		
Site 3-60cm	0.411		0.402	0.408		
Site 3-90cm	0.406		0.398	0.391		
Site 3-120cm	0.397		0.384	0.371		
Site 4-30cm	0.341		0.334	0.327		
Site 4-60cm	0.433		0.420	0.404		
Site 4-90cm	0.390		0.377	0.368		
Site 4-120cm	0.412		0.394	0.384		
Site 5-30cm		0.258		0.242		0.198
Site 5-60cm		0.451		0.434		0.391
Site 5-90cm		0.420		0.404		0.349
Site 5-120cm		0.391		0.371		0.289

Table 9. Field 4 desorption soil-moisture retention data. Values are volumetric water content.

	Pressure (-kPa)								
	3.103	9.810	9.997	10.342	30.682	49.987	51.366	99.975	293.029
Site 1-30cm	0.345		0.322			0.300		0.299	0.288
Site 1-60cm	0.392		0.380			0.363		0.356	0.348
Site 1-90cm	0.404		0.395			0.390		0.389	0.383
Site 1-120cm	0.442		0.429			0.417		0.406	0.398
Site 2-30cm	0.322		0.296			0.272		0.262	0.246
Site 2-60cm	0.386		0.375			0.361		0.364	0.356
Site 2-90cm	0.433		0.419			0.410		0.402	0.394
Site 2-120cm	0.427		0.406			0.366		0.359	0.355
Site 3-30cm	0.364		0.339			0.317		0.313	0.297
Site 3-60cm	0.430		0.416			0.405		0.402	0.387
Site 3-90cm	0.402		0.393			0.383		0.383	0.379
Site 3-120cm	0.427		0.415			0.396		0.395	0.386
Site 4-30cm	0.386			0.367			0.332	0.324	0.298
Site 4-60cm	0.403			0.373			0.348	0.333	0.308
Site 4-90cm	0.439			0.414			0.405	0.401	0.382
Site 4-120cm	0.455			0.431			0.414	0.415	0.397
Site 5-30cm	0.366	0.337			0.303		0.281	0.250	
Site 5-60cm	0.425	0.411			0.391		0.377	0.358	
Site 5-90cm	0.457	0.451			0.439		0.432	0.419	
Site 5-120cm	0.479	0.473			0.448		0.416	0.377	

Table 9 cont.

	296.476
Site 1-30cm	
Site 1-60cm	
Site 1-90cm	
Site 1-120cm	
Site 2-30cm	
Site 2-60cm	
Site 2-90cm	
Site 2-120cm	
Site 3-30cm	
Site 3-60cm	
Site 3-90cm	
Site 3-120cm	
Site 4-30cm	
Site 4-60cm	
Site 4-90cm	
Site 4-120cm	
Site 5-30cm	0.20
Site 5-60cm	0.31
Site 5-90cm	0.38
Site 5-120cm	0.30